

# Exploring the impact of UV-C radiation and UV-protective additives on SEBS thermoplastic materials

Ahmet Güngör<sup>1,2</sup> , Dilek Turan<sup>3</sup>, Şerif Erdoğan<sup>3</sup>  
 and Tonguç Özdemir<sup>4,5</sup>

Plastics, Rubber and Composites

1–9

© The Author(s) 2025

Article reuse guidelines:

sagepub.com/journals-permissions

DOI: 10.1177/14658011251349030

journals.sagepub.com/home/prc



## Abstract

Styrene-ethylene-butylene-styrene (SEBS) thermoplastic elastomers are highly sought after for various industrial and consumer applications due to their exceptional flexibility, impact resistance, and thermal stability. However, their susceptibility to ultraviolet (UV) degradation, particularly from UV-C radiation, significantly challenges their long-term performance. This study investigates the impact of UV-C radiation on SEBS and evaluates the effectiveness of a UV protective additive in mitigating these effects. Neat SEBS and UV-protected SEBS samples were subjected to accelerated UV-C weathering for 2 weeks, and their mechanical, thermal, morphological, and chemical properties were thoroughly characterised before and after exposure. The results demonstrate that UV-C radiation significantly reduces the tensile strength of neat SEBS and induces nano-crack formation on its surface, as revealed by mechanical testing and scanning electron microscopy analysis, respectively. Furthermore, UV-C exposure negatively affects the thermal stability of SEBS, as evidenced by a decrease in the  $T_{50}$  temperature determined from thermogravimetric analysis. However, incorporating the UV-protective additive significantly mitigates these detrimental effects. The UV-protected SEBS retains a much higher percentage of its original tensile strength, exhibits minimal changes in surface morphology, and maintains comparable thermal stability to the unexposed samples. These findings highlight the crucial role of UV protective additives in enhancing the resistance of SEBS to UV-C radiation, paving the way for developing more durable and weather-resistant SEBS materials for demanding applications.

## Keywords

styrene-ethylene-butadiene-styrene (SEBS), UV-protective additive, UV-C radiation, thermal analysis

Received: 24 September 2024; accepted: 25 May 2025

## Introduction

Thermoplastic elastomers (TPEs) represent a versatile polymeric material class bridging the gap between conventional and rigid thermoplastics. This unique characteristic stems from their ability to exhibit elastomeric behaviour at ambient temperatures while retaining the ability to be processed like thermoplastics at elevated temperatures.<sup>1–4</sup> Among the various types of TPEs, styrene-ethylene-butylene-styrene (SEBS) block copolymers have garnered significant attention due to their exceptional combination of properties, including excellent flexibility, impact resistance, thermal stability, chemical resistance, and adhesion properties.<sup>5–7</sup>

SEBS is a triblock copolymer characterised by a unique molecular architecture consisting of two terminal polystyrene (S) blocks, which impart rigidity, and a central poly(ethylene-co-butylene) (EB) block, which contributes to the material's elastomeric nature.<sup>8–10</sup> This microphase-separated morphology, where the rigid polystyrene domains are dispersed within a continuous rubbery EB matrix, is responsible for the remarkable properties of SEBS, making

it suitable for a wide range of applications in various industries, including automotive, medical, packaging, electronics, and textiles<sup>11–13</sup>.

Despite their versatility and desirable properties, SEBS materials are susceptible to degradation when exposed to environmental factors, particularly ultraviolet (UV) radiation.<sup>14–16</sup> UV radiation, a high-energy form of electromagnetic radiation, can initiate photo-oxidative degradation

<sup>1</sup>Faculty of Engineering and Natural Sciences, Sabancı University, Tuzla, Istanbul, Turkey

<sup>2</sup>Center of Excellence for Functional Surfaces and Interfaces for Nano-Diagnostics (EFSUN), Sabancı University, Tuzla, Istanbul, Turkey

<sup>3</sup>Elastron TPE Industry and Trade Inc., Gebze, Kocaeli, Turkey

<sup>4</sup>Chemical Engineering Department, Mersin University, Mersin, Turkey

<sup>5</sup>Advanced Technology Education Research and Application Center, Mersin University, Mersin, Turkey

## Corresponding author:

Ahmet Güngör, Address: Sabancı University, 34956, Orhanlı, Tuzla, İstanbul, Turkey.

Email: ahmet.gungor@sabanciuniv.edu

processes within the SEBS matrix, leading to chain scission, crosslinking, and the formation of free radicals.<sup>17–19</sup> UV radiation is classified into three categories based on wavelength: UV-A (315–400 nm), UV-B (280–315 nm), and UV-C (100–280 nm).<sup>20</sup> UV-A radiation, with the longest wavelength and lowest energy, primarily causes surface-level effects such as discolouration and minor degradation in polymers.<sup>21</sup> UV-B radiation, with intermediate energy, can penetrate deeper into the polymer matrix, leading to more significant degradation, including chain scission and crosslinking.<sup>22</sup> UV-C radiation, with the shortest wavelength and highest energy, is the most damaging to polymers. It induces severe photo-oxidative degradation, resulting in the formation of free radicals, chain scission, and structural changes.<sup>23</sup> While UV-C radiation is primarily filtered by the Earth's atmosphere, it is commonly used in artificial environments for sterilisation and accelerated weathering tests, making it a critical focus for understanding polymer durability under extreme conditions. These photochemical reactions result in undesirable changes in the material's properties, such as reduced mechanical strength, loss of elasticity, discolouration, and surface cracking, ultimately compromising its performance and limiting its long-term durability, especially in outdoor applications.<sup>17–19,24</sup>

To mitigate the detrimental effects of UV radiation on SEBS, UV stabiliser additives are commonly incorporated into the polymer matrix.<sup>25–27</sup> These stabilisers function by absorbing harmful UV radiation and converting it into less dangerous forms of energy, such as heat, effectively shielding the SEBS from photodegradation and extending its service life.<sup>28–30</sup> UV stabilisers can be categorised into two main types: UV absorbers, which primarily absorb UV radiation, and hindered amine light stabilisers (HALS), which function as radical scavengers, interrupting the photo-oxidation cycle and preventing further degradation.<sup>31,32</sup>

This study aims to investigate the effects of UV-C radiation, a particularly damaging form of UV radiation, on the properties of SEBS thermoplastic materials and to evaluate the effectiveness of UV protective additives in mitigating these effects. To this end, neat SEBS samples and SEBS samples containing a UV protective additive were subjected to accelerated UV-C weathering for 2 weeks. The materials' mechanical properties, thermal stability, surface morphology, and chemical structure were characterised before and after UV-C exposure to assess

the extent of degradation and the protective effect of the UV stabiliser. The findings of this study will provide valuable insights into the photodegradation behaviour of SEBS and the role of UV protective additives in enhancing its resistance to UV radiation, contributing to the development of more durable and weather-resistant SEBS materials for demanding applications.

## Material & method

### Materials

The study utilised neat SEBS and UV-protective doped SEBS composite materials provided by Elastron TPE Industry and Trade Inc. (production code RD.444.907). The neat SEBS sample refers to the base SEBS material in its pure form, without any additional stabilisers or UV-protective additives. It was used as a control to evaluate the effects of UV-C radiation on the unprotected SEBS matrix. This sample was used as a control to assess the impact of UV-C radiation on the unprotected SEBS matrix. The products were produced for medical use and manufactured according to ASTM standards. Table 1 displays the samples and contents obtained from Elastron TPE. The SEBS block copolymer, containing 30% styrene and 70% ethylene-butylene, was sourced from the TSRC Company (Taiwan). This high styrene content ensures a balanced combination of rigidity and elastomeric flexibility, which is critical for assessing degradation behaviour under 'UV-C' stress.

The process oil used in the formulation is paraffinic-based with a viscosity of 70 cSt at 40°C, supplied by Petroyağ Company (Türkiye). The homo-PP component has a melt flow index of 1.8 g/10 min (230°C/2.16 kg) and was obtained from Lyondell Basell (Holland). The master batch, which is polyethylene and carbon black-based, was provided by Sisan Masterbatch (Türkiye). The inclusion of carbon black also contributes to minor UV shielding and acts as a pigmenting agent, enhancing the visual contrast of surface degradation effects.

As UV-protective additives, a phenolic antioxidant was used for processing and long-term stabilisation, a benzotriazole-based UV absorber was incorporated to absorb harmful UV radiation, and a HALS based on tetramethyl piperidine derivatives was added to scavenge free radicals. All additives were sourced from BASF (Germany). The combined use of UVA and HALS creates

**Table I.** The used SEBS-based samples and their contents.

Sample	UV-protective additive	Hardness (Shore A)	Description
SEBS	No	60	Neat SEBS without any stabilisers or UV-protective additives (control sample).
SEBS-Add	Yes	60	SEBS with UV-protective additives (UVA and HALS) for enhanced UV resistance.
SEBS@UVC	No	60	Neat SEBS exposed to UV-C radiation for 2 weeks.
SEBS-Add@UVC	Yes	60	SEBS with UV-protective additives exposed to UV-C radiation for 2 weeks.

SEBS: styrene-ethylene-butylene-styrene; UV: ultraviolet; HALS: hindered amine light stabilisers.

a synergistic protection mechanism, where UVA prevents photon penetration and HALS interrupts the degradation cycle by neutralising formed radicals. This dual-mode stabilisation is particularly effective against high-energy UV-C radiation, which causes both surface and bulk degradation.

The materials were blended in a mixer for 10 min to ensure homogeneity. Proper mixing was essential to ensure uniform dispersion of the additives throughout the polymer matrix, which directly affects their protective efficiency. The compounds were then processed using a co-rotating twin-screw extruder at 300 rpm, with a temperature profile of 140 °C (feed zone), 150–180 °C (melting zones), and 190 °C (die zone). This extrusion profile was optimised to prevent thermal degradation of the antioxidant and UV stabilisers. The final samples were prepared according to ASTM standards for subsequent mechanical, thermal, morphological, and chemical analyses.

### **Characterisation of SEBS-based composite materials**

The mechanical characteristics of composite materials were evaluated by the ASTM D412 standard using a Shimadzu-AGS X model universal testing machine. Within this framework, mechanical analyses were performed by dissecting the samples into bow-tie shapes. Thermogravimetric analysis (TGA) was used to evaluate the thermal stability of SEBS and SEBS-based composite materials. Differential mechanical analysis (DMA) was employed to determine the viscoelastic properties of the composites. The TGA analysis was performed using a TA Instruments SDT 650 Simultane DSC/TGA instrument in a nitrogen atmosphere. The temperature range was configured to span from 25 to 800 °C, with a heating rate of 20 °C/min. An analysis was performed using the DMA technique (Perkin Elmer-Pyris Diamond) over a temperature range of –90 to 150 °C. The analysis was conducted with a frequency of 1 Hz and a heating rate of 5 °C/min. Also, differential scanning calorimetry (DSC) was used to characterise the materials' glass transition temperature ( $T_g$ ) value. DSC and TGA analysis were performed simultaneously on TA Instruments SDT 650 Simultaneous DSC/TGA device. An fourier transform infrared spectroscopy (FTIR) examination was performed using Thermo Scientific iS50 equipment to evaluate the functional groups within the prepared composite materials. The FTIR spectrum of the prepared composites was acquired by conducting 64 scans with a resolution of 2  $\text{cm}^{-1}$ . The scanning electron microscopy (SEM) analysis, explicitly using the QUANTA-650 model, was conducted to investigate the cross-sectional surface morphology of the prepared composites. The objective was to assess the influence of incorporating UV additives. Concerning this issue, the prepared composites were subjected to a platinum coating, and images of different magnitudes were captured.

Eventually, the neat SEBS and SEBS-Add samples were exposed to UV-C radiation for 2 weeks. After 2 weeks, an analysis was conducted to evaluate all samples' thermal, mechanical, morphological, and chemical characteristics, specifically investigating the impact of irradiation.

### **Results & discussion**

This study characterised the mechanical, thermal, and morphological properties of neat SEBS and UV-protective doped SEBS composites. In addition, the post-exposure mechanical, thermal, and surface morphological changes of the samples exposed to UV-C irradiation at the same doses (for 2 weeks) were investigated.

### **FTIR analysis**

The nature, composition, and production method of olefin starting materials determine the complicated structure of SEBS block copolymer. The ethylene-butylene copolymer that makes up the elastomeric unit is hydrogenated from a butadiene precursor. The units often have a distinct chemical border between the 'polystyrene' and 'elastomer' components, resulting in an incompatible stage. Sites are evenly distributed when the polystyrene content is below 50%. FTIR spectroscopy was employed to investigate the chemical structure and potential structural changes in SEBS and SEBS-Add composites before and after UV-C irradiation. Figure 1 presents the FTIR spectra of the neat SEBS, SEBS-Add, SEBS@UVC, and SEBS-Add@UVC samples.

The FTIR spectrum of the neat SEBS sample exhibits characteristic peaks associated with its molecular structure. The prominent peaks observed between 1601 and 1452  $\text{cm}^{-1}$  correspond to the aromatic C=C stretching vibrations of the phenyl rings in the polystyrene blocks.<sup>33</sup> The peaks at 757  $\text{cm}^{-1}$  and 698  $\text{cm}^{-1}$  are attributed to the C-H bending vibrations of the monosubstituted benzene rings, further confirming the presence of polystyrene.<sup>33,34</sup> The peak at 1378  $\text{cm}^{-1}$  is assigned to the C-H bending vibration of the methylene groups in the EB segments.<sup>34,35</sup> The spectral region between 1300 and 1200  $\text{cm}^{-1}$  exhibits peaks related to the butadiene region, indicating the presence of the styrene-butadiene block.<sup>36</sup> This region also includes C-H bending modes of styrene.<sup>36</sup> The minor

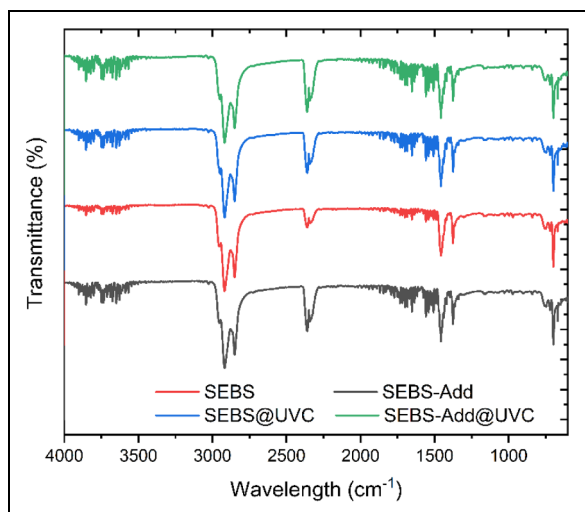


**Figure 1.** FTIR analysis of SEBS and SEBS-Add sample before and after UV-C irradiation .SEBS: styrene-ethylene-butylene-styrene; UV: ultraviolet.

peaks with low intensity observed at  $1031\text{ cm}^{-1}$  correspond to C–H bending modes, indicating specific groups in the styrene and ethylene regions.<sup>34,35</sup>

Upon exposure to UV-C radiation, the SEBS sample (SEBS@UVC) exhibits noticeable changes in its FTIR spectrum. The intensity of the peaks in the  $1601\text{--}1452\text{ cm}^{-1}$  region, associated with aromatic C=C stretching vibrations, decreases, suggesting some degree of photo-oxidation of the styrene units. This observation is consistent with the known susceptibility of aromatic rings to UV-induced degradation. Additionally, increased noise and broadened peaks are observed in the  $1500\text{--}1350\text{ cm}^{-1}$  and  $1350\text{--}1200\text{ cm}^{-1}$  ranges, typically associated with alkene groups.<sup>33–35</sup> This suggests possible chain scission and the formation of new unsaturated groups due to UV-C exposure.

In contrast to the neat SEBS sample, the SEBS-Add sample, containing the UV protective additive, shows minimal changes in its FTIR spectrum after UV-C irradiation (SEBS-Add@UVC). The intensity of the peaks associated with aromatic C=C stretching vibrations remains relatively unchanged, indicating that the UV protective additive effectively shields the styrene units from photo-oxidation. Furthermore, no significant increase in noise or peak broadening is observed in the alkene regions, suggesting that the UV protective additive also inhibits chain scission and the formation of new unsaturated groups. The FTIR analysis confirms the presence of the expected functional groups in both SEBS and SEBS-Add composites. Moreover, the results demonstrate that UV-C irradiation leads to structural changes in the neat SEBS, primarily affecting the styrene units. However, incorporating the UV protective additive effectively mitigates these structural changes, preserving the chemical integrity of the SEBS-Add composite upon UV-C exposure.

### Mechanical analysis

The mechanical properties of the provided SEBS and UV-protective doped SEBS (SEBS-Add) samples were analysed before and after exposure to UV-C radiation. The results of the analysis are summarised in Table 2. Upon examination of the values before UV-C exposure, it is evident that adding a UV-protective additive to the SEBS matrix enhances the material's tensile strength and modulus of elasticity. An incomplete reduction was noted in the elongation at break measurement. Following exposure to UV-C irradiation, the mechanical properties of both samples decreased as anticipated. The impact of the UV-C protective additive is evident through the mechanical analysis results. The tensile strength of the sample without added UV protection decreased by approximately 25%. However, in the sample with UV-C added (SEBS-Add@UVC), this decrease was only around 8%. This indicates that the UV-C protective additive effectively maintained the tensile strength, as observed in the mechanical analysis results. An analogous scenario can be observed in the extent of elongation at the fracture point. Following exposure to UV-C irradiation, the elongation of SEBS

**Table 2.** Mechanical analysis of SEBS and SEBS-Add sample before and after UV-C irradiation.

Sample	Tensile strength at break MPa	Mod. of elasticity % 100 MPa	Elongation at break %
SEBS	$8.44 \pm 0.52$	$1.92 \pm 0.07$	$985 \pm 52$
SEBS-Add	$8.62 \pm 0.44$	$1.98 \pm 0.08$	$940 \pm 46$
SEBS@UVC	$6.42 \pm 0.28$	$1.64 \pm 0.05$	$855 \pm 31$
SEBS-Add@UVC	$7.94 \pm 0.36$	$1.76 \pm 0.05$	$896 \pm 34$

SEBS: styrene-ethylene-butylene-styrene; UV: ultraviolet.

decreased from 985% to 855%. However, in the SEBS-Add example, this reduction only reduced from 940% to approximately 900%. It is anticipated that following exposure to UV-C radiation, there will be a reduction in both the SEBS matrix and the surface morphology, consequently affecting its mechanical properties. This study found that adding a UV-C protective additive to the SEBS matrix effectively maintained its mechanical properties when exposed to radiation.

### Thermal analysis

TGA was conducted to investigate the thermal stability of the neat SEBS, SEBS-Add, SEBS@UVC, and SEBS-Add@UVC samples. The TGA curves, representing the weight loss of the samples as a function of temperature, are presented in Figure 2(a). The TGA curves of all samples exhibit a similar multi-stage degradation profile, which is characteristic of SEBS block copolymers. The initial weight loss observed between 25 and 200 °C can be attributed to the desorption of residual volatiles, such as moisture absorbed during processing and low molecular weight oligomers.<sup>37</sup> The second stage of degradation, occurring between 200 and 400 °C, is characterised by a more significant weight loss and corresponds to the cleavage of chemical bonds within the SEBS structure. This temperature range aligns with the reported degradation temperatures for the poly(ethylene-co-butylene) (EB) segments in SEBS.<sup>38,39</sup> The degradation of EB likely involves random chain scission reactions, leading to the formation of volatile hydrocarbons. The third and final stage of degradation, observed between 400 and 600 °C, is attributed to the decomposition of the polystyrene (PS) blocks.<sup>38,40</sup> The degradation of PS typically proceeds through depolymerisation reactions, resulting in the formation of styrene monomers and other volatile aromatic compounds.<sup>24</sup>

Upon closer examination of the TGA curves, it is evident that adding the UV protective additive positively impacts the thermal stability of SEBS. The SEBS-Add sample exhibits a slightly higher onset temperature for the second degradation stage than the neat SEBS, indicating enhanced resistance to thermal degradation. This improvement can be attributed to the ability of the UV protective additive to scavenge free radicals generated during thermal degradation, thereby delaying the onset of significant weight loss.

Furthermore, the TGA results reveal that UV-C irradiation has a more pronounced effect on the neat SEBS's thermal stability than the SEBS-Add sample. The residual mass exceeding 8% observed in the SEBS sample after TGA analysis can be attributed to the formation of a carbonaceous char during the thermal degradation process. Under the inert nitrogen atmosphere used in the analysis, some degradation products, particularly from the polystyrene (PS) segments, may undergo secondary reactions such as cross-linking or cyclisation, resulting in a thermally stable residue. This phenomenon is consistent with previous studies on the thermal degradation of SEBS and similar block copolymers.<sup>34,41</sup> The SEBS@UVC sample exhibits a lower onset temperature for the second degradation stage and a higher weight loss rate than the neat SEBS, suggesting that UV-C irradiation accelerates the thermal degradation process. This observation is consistent with the FTIR analysis, which indicated photo-oxidation and chain scission in the neat SEBS upon UV-C exposure. In contrast, the SEBS-Add@UVC sample exhibits comparable thermal stability to the SEBS-Add sample, indicating that the UV protective additive effectively mitigates the detrimental effects of UV-C radiation on the thermal stability of SEBS. The UV protective additive likely absorbs the harmful UV-C radiation, preventing it from reaching the SEBS matrix and initiating photo-oxidative degradation processes.

The  $T_{50}$  temperatures, representing the temperature at which 50% of the initial weight is lost, provide further insights into the thermal stability of the samples. The SEBS@UVC sample exhibits the lowest  $T_{50}$  temperature (approximately 430 °C), indicating the most significant degradation due to UV-C exposure. The neat SEBS and SEBS-Add@UVC samples exhibit similar  $T_{50}$  temperatures (around 440 °C), suggesting comparable thermal stability. The SEBS-Add sample exhibits the highest  $T_{50}$  temperature (approximately 441 °C), indicating the highest thermal stability among the tested samples.

DSC was employed to investigate the thermal transitions and thermal behaviour of the neat SEBS, SEBS-Add, SEBS@UVC, and SEBS-Add@UVC samples. The DSC curves, representing the heat flow as a function of temperature, are presented in Figure 2(b). The DSC curve of the neat SEBS sample reveals several key thermal event characteristics of its microphase-separated structure. The endothermic peak observed at approximately 25 °C corresponds to the glass transition temperature ( $T_g$ ) of the poly(ethylene-co-butylene) (EB) phase. This transition signifies the EB phase softening from a rigid, glassy state to a more flexible, rubbery state.<sup>42</sup>

The addition of the UV protective additive (SEBS-Add) results in a slight increase in  $T_g$  to -51 °C, suggesting that the additive enhances the interaction between the SEBS blocks, leading to a slightly more restricted molecular mobility.<sup>15,43</sup> After UV-C irradiation, the  $T_g$  values of both SEBS@UVC and SEBS-Add@UVC samples exhibit a slight increase, as determined from the tan delta peaks. This increase in  $T_g$  can be attributed to photo-oxidation and crosslinking reactions induced by UV-C exposure,

which restrict molecular mobility.<sup>42,44</sup> However, the changes in  $T_g$  are minimal, particularly for the SEBS-Add@UVC sample, indicating that the UV protective additive effectively mitigates the structural changes typically induced by UV-C radiation.

The broad endothermic peak observed between 200 and 250 °C can be attributed to the melting of crystalline domains within the EB phase.<sup>39–41</sup> While not as common in copolymers, the ethylene and butylene units in the EB chains can exhibit a certain degree of regularity, allowing them to pack into ordered crystalline structures. This melting peak indicates the breakdown of these ordered regions, leading to a transition to a completely amorphous state. This melting peak remains unchanged mainly after UV-C exposure, further confirming the protective effect of the UV additive in preserving the thermal integrity of the SEBS matrix. Contrary to the endothermic peaks observed at lower temperatures, an exothermic peak emerges at approximately 300 °C. This exothermic event suggests that the SEBS polymer is undergoing thermal degradation or crosslinking reactions. This could involve decomposing thermally unstable groups within the polymer chains or forming new chemical bonds between chains, leading to crosslinking. Finally, a significant exothermic peak is observed between 430 and 500 °C, indicating the complete thermal decomposition or carbonisation of the SEBS polymer.<sup>38,41,42</sup> The SEBS undergoes irreversible chemical changes at this temperature range, breaking down into smaller, volatile degradation products and leaving behind a residual carbonaceous char.

DMA was employed to investigate the viscoelastic properties of neat SEBS, SEBS-Add, SEBS@UVC, and SEBS-Add@UVC samples over various temperatures. Figure 3 presents the storage modulus ( $E'$ ), loss modulus ( $E''$ ), and tan delta ( $\tan \delta$ ) curves obtained from DMA measurements. The storage modulus ( $E'$ ) reflects the material's stiffness and ability to store elastic energy during deformation. All samples exhibit a high storage modulus at low temperatures, which is characteristic of a glassy, rigid state. As the temperature rises, the storage modulus gradually decreases, indicating a softening of the material as it transitions toward a more rubbery state. Adding the UV protective additive appears to increase the storage modulus slightly at low temperatures, suggesting a possible enhancement in stiffness. However, this effect diminishes as the temperature rises, and the storage modulus curves for all samples converge at higher temperatures.

The loss modulus ( $E''$ ) represents the energy dissipated as heat during deformation, providing insights into the viscous behaviour of the material. The loss modulus curves for all samples exhibit a prominent peak, known as the alpha relaxation peak, which corresponds to the glass transition temperature ( $T_g$ ) of the EB phase.<sup>11,44</sup> This peak reflects the increased molecular mobility and energy dissipation associated with the transition from a glassy to a rubbery state. Interestingly, adding the UV protective additive appears to shift the onset of the alpha relaxation peak to a slightly lower temperature, suggesting a possible plasticising effect of the additive on the EB phase.

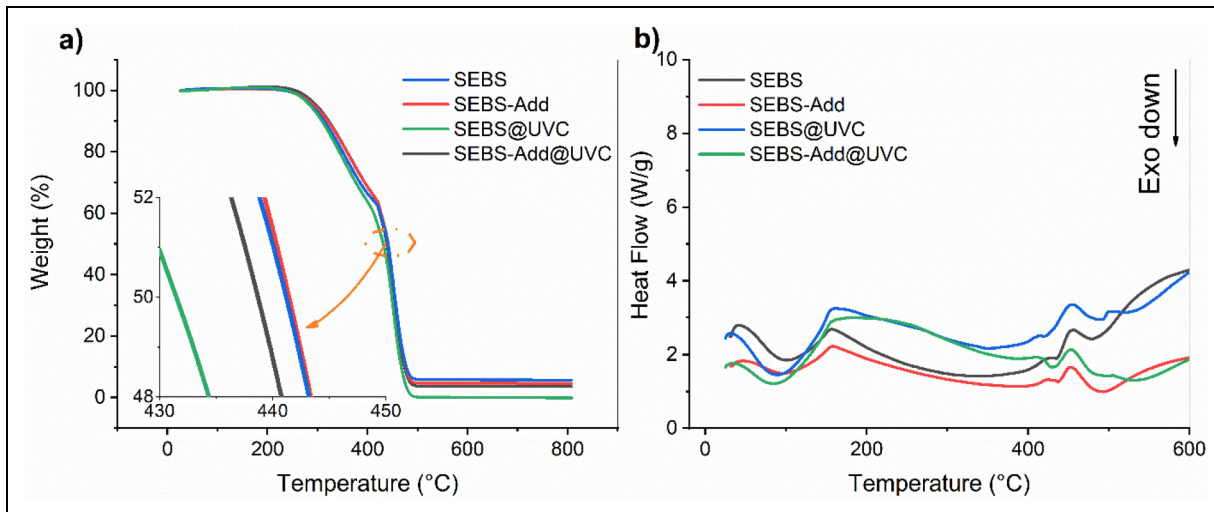


**Figure 2.** (a) TGA and (b) DSC analysis of SEBS and SEBS-Add samples before and after UV-C irradiation. SEBS: styrene-ethylene-butylene-styrene; UV: ultraviolet; TGA: thermogravimetric analysis; DSC: differential scanning calorimetry.

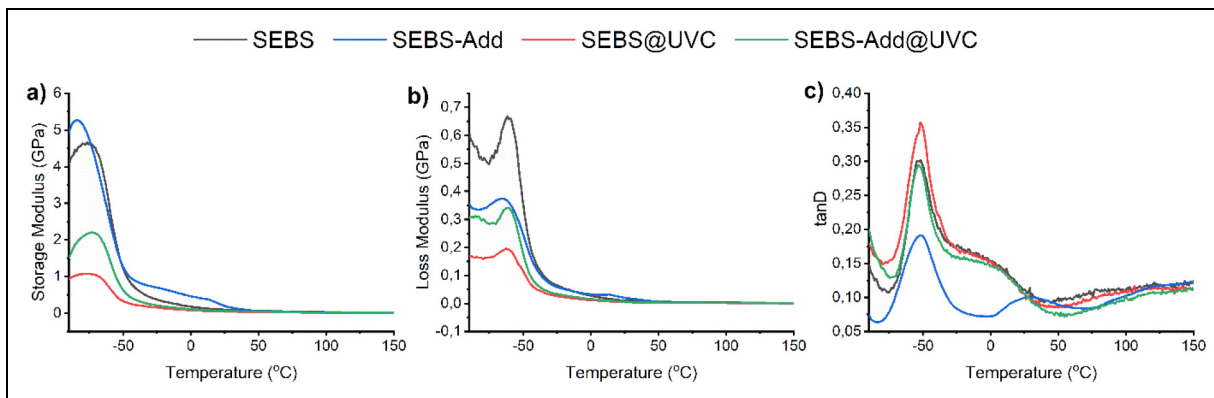


**Figure 3.** DMA analysis of SEBS and SEBS-Add sample before and after UV-C irradiation. SEBS: styrene-ethylene-butylene-styrene; UV: ultraviolet; DMA: differential mechanical analysis.

The  $\tan \delta$  is the ratio of the loss modulus to the storage modulus ( $E''/E'$ ). It measures the material's damping behaviour, indicating its ability to dissipate energy during cyclic loading. The  $\tan \delta$  curves exhibit a peak at  $T_g$ , reflecting the maximum energy dissipation at this transition. The neat SEBS sample exhibits a  $T_g$  of approximately  $-53.12^\circ\text{C}$ , as determined from the  $\tan \delta$  peak. The addition of the UV protective additive (SEBS-Add) results in a slight increase in the  $T_g$  to  $-51^\circ\text{C}$ , suggesting that the additive may enhance the interaction between the SEBS blocks, leading to a slightly more restricted molecular mobility.<sup>15,43</sup> After UV-C irradiation, the SEBS@UVC and SEBS-Add@UVC samples exhibit a slight increase in their  $T_g$  values, as determined from the  $\tan \delta$  peaks. This increase in  $T_g$  can be attributed to photo-oxidation and crosslinking reactions induced by UV-C irradiation, leading to a more restricted molecular mobility.<sup>15,42-44</sup>

#### Surface morphology of SEBS composites

SEM analysis examined the surface morphologies of SEBS and UV-protectant-added SEBS samples before

and after irradiation. The resulting SEM scans can be seen in Figure 4. Upon examination, the surface morphology of pure SEBS reveals a highly uniform and sleek surface. The SEM scans of the SEBS-Add sample, created by incorporating a UV-protective additive into the SEBS structure, indicate that the additive material is uniformly distributed throughout the matrix and is easily visible on the material's surface. Upon examination of the surface morphologies of both samples following irradiation, it is evident that the surface of the SEBS-Add@UVC sample remains unaffected by UV-C radiation, with no occurrence of deformation. The changes in surface morphology due to UV-C exposure were investigated using SEM analysis, as shown in Figure 4. The SEM images reveal the formation of nano-cracks on the surface of the neat SEBS sample after UV-C exposure, while the UV-protected SEBS sample remains unaffected. These observations provide visual evidence of the structural damage caused by UV-C radiation and its mitigation by the UV protective additive. Nevertheless, in the SEBS@UVC sample, cracks were observed at the nanoscale, as evidenced by the yellow rings.

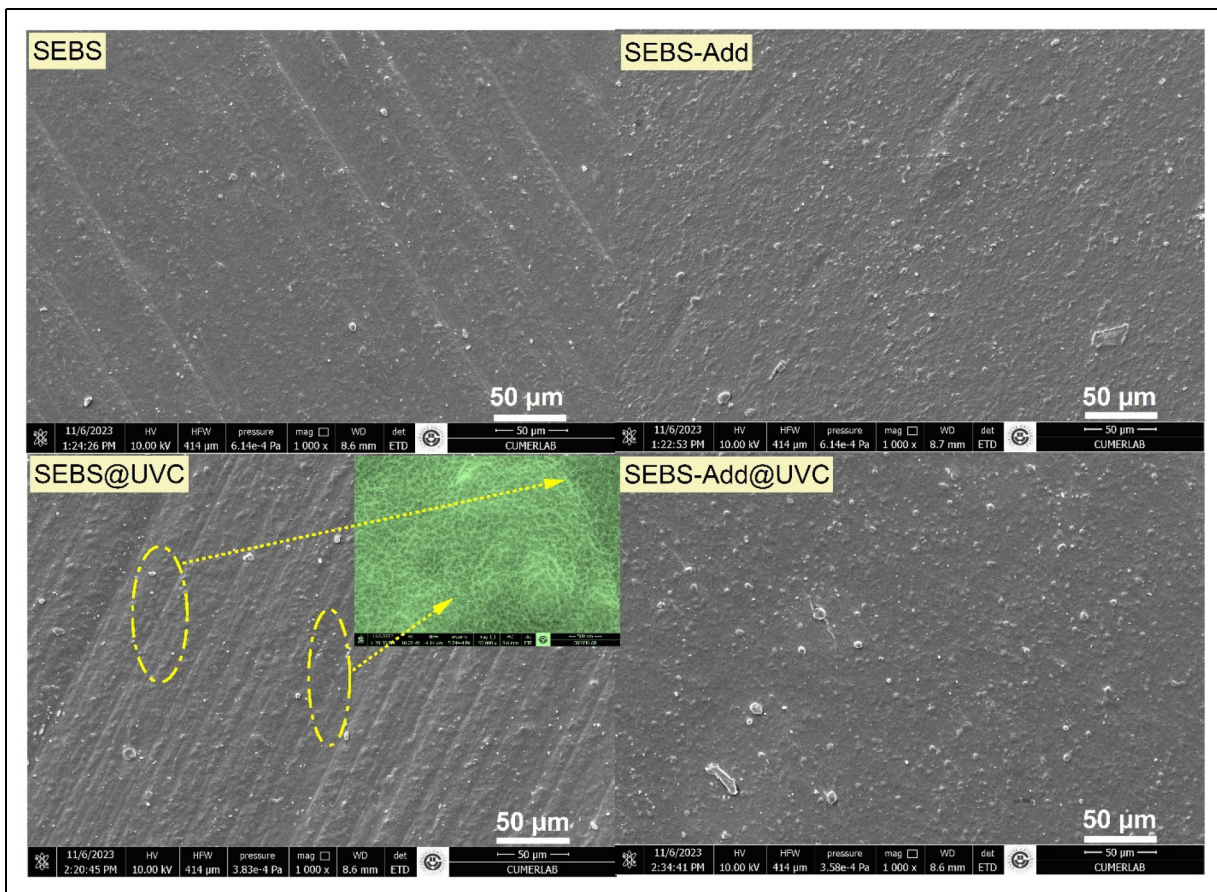


**Figure 4.** SEM images of SEBS and SEBS-Add samples before and after UV-C irradiation. The surface morphology of the neat SEBS sample (SEBS@UVC) reveals the formation of nano-cracks (highlighted by yellow rings) after UV-C exposure, while the UV-protected SEBS sample (SEBS-Add@UVC) remains unaffected. SEBS: styrene-ethylene-butylene-styrene; UV: ultraviolet; SEM: scanning electron microscopy.

## Conclusion

SEBS is a versatile TPE with a wide range of applications. It exhibits excellent flexibility, impact resistance, chemical resistance, thermal stability, and adhesion properties. However, its susceptibility to UV degradation, particularly from UV-C radiation, poses a significant challenge to its long-term performance in outdoor applications. This study investigated the effects of UV-C radiation on SEBS and the effectiveness of a UV protective additive in mitigating these effects. The results of this study demonstrate that prolonged exposure to UV-C radiation leads to a significant deterioration in the mechanical properties of neat SEBS. Specifically, a 25% reduction in tensile strength was observed after 2 weeks of UV-C irradiation. This decline in mechanical performance can be attributed to the photo-oxidative degradation processes initiated by UV-C radiation, leading to chain scission, crosslinking, and the formation of free radicals within the SEBS matrix. These chemical changes disrupt the structural integrity of SEBS, resulting in reduced tensile strength and other undesirable mechanical changes. SEM analysis corroborated the mechanical testing results, revealing the formation of nano-cracks on the surface of the neat SEBS samples after UV-C irradiation. These nano-cracks act as stress

concentrators, weakening the material and making it more susceptible to fracture under tensile stress. The observed nano-cracks provide visual evidence of the structural damage inflicted upon SEBS by UV-C radiation. Furthermore, the thermal stability of SEBS was negatively impacted by UV-C exposure. The  $T_{50}$  temperature, representing the temperature at which 50% weight loss occurs, decreased from 440 °C to 430 °C after UV-C irradiation, indicating a reduction in thermal stability. This finding suggests that UV-C radiation accelerates the thermal degradation processes in SEBS, leading to an earlier onset of decomposition and weight loss. However, incorporating a UV-protective additive into the SEBS matrix mitigated UV-C radiation's detrimental effects. The UV-protected SEBS exhibited significantly higher tensile strength retention (only a 7% decrease) after UV-C irradiation compared to the neat SEBS. Moreover, the UV-protected SEBS showed minimal changes in its surface morphology and thermal stability after UV exposure, confirming the effectiveness of the additive in preserving the material's structural integrity.

This study highlights the importance of considering the detrimental effects of UV radiation when selecting SEBS for outdoor applications. The findings demonstrate that incorporating a UV-protective additive can significantly

enhance SEBS's resistance to UV-C radiation, preserving its mechanical properties, surface morphology, and thermal stability. This study provides valuable insights for developing more durable and weather-resistant SEBS materials for demanding applications, contributing to the advancement of polymer technology for enhanced material longevity and performance. While this study provides a comprehensive analysis of the effects of UV-C radiation on SEBS, the reduction in the SEBS matrix was not quantified using gel permeation chromatography (GPC), as GPC analysis was not included in the experimental design of this study. Future studies should incorporate GPC analysis to quantify molecular weight changes and establish a more robust structure-performance correlation.

### Acknowledgment

The authors would like to thank Elastron TPE Industry and Trade Inc. for their valuable contributions to providing the materials.

### Data availability statement

The raw/processed data required to reproduce these findings cannot be shared at this time

### Declaration of conflicting interests

The authors declared no potential conflicts of interest with respect to the research, authorship, and/or publication of this article.

### Funding

The authors received no financial support for the research, authorship, and/or publication of this article.

### ORCID iD

Ahmet Güngör  <https://orcid.org/0000-0002-8319-1652>

### References

- Costa FR, Dutta NK, Choudhury NR, et al. Thermoplastic elastomers. In: *Current topics in ELASTOMERS RESEARCH*. Boca Raton, FL: CRC Press, 2008, pp.101–164.
- Holden G. Thermoplastic elastomers. In: *Applied plastics engineering handbook*. Norwich, NY: William Andrew Publishing, 2024, pp.97–113.
- Legge NR. Thermoplastic elastomers—three decades of progress. *Rubber Chem Technol* 1989; 62: 529–547. Allen Press.
- Whelan D. Thermoplastic elastomers. In: *Brydson's plastics materials. 8th ed.* Oxford: Elsevier, 2017, pp.653–703.
- Adhikari R and Michler GH. Influence of molecular architecture on morphology and micromechanical behavior of styrene/butadiene block copolymer systems. *Prog Polym Sci* 2004; 29: 949–986. Pergamon.
- Paria S, Mondal S, Lee GB, et al. TPE Nanocomposites; processing and additives. In: *Advances in thermoplastic elastomers: challenges and opportunities*. Amsterdam: Elsevier, 2024, pp.445–472.
- Shin J, Kim YW and Kim GJ. Sustainable block copolymer-based thermoplastic elastomers. *Appl Chem Eng* 2014; 25: 121–133.
- Crawford EA, Gupta S, Trinh BM, et al. Styrene-ethylene-butylene-styrene (SEBS) melt-blown fibers for oil spill remediation and oil barrier geotextiles. *Polymer* 2024; 298: 126942. Elsevier.
- Rickert R, Klein R and Schönberger F. Form-stable phase change materials based on SEBS and paraffin: influence of molecular parameters of styrene-b-(ethylene-co-butylene)-b-styrene on shape stability and retention behavior. *Materials (Basel)* 2020; 13: 3285. Multidisciplinary Digital Publishing Institute.
- Veenstra H, Van Lent BJJ, Van Dam J, et al. Co-continuous morphologies in polymer blends with SEBS block copolymers. *Polymer* 1999; 40: 6661–6672. Elsevier.
- Gupta AK and Purwar SN. Dynamic mechanical and impact properties of PP/SEBS blend. *J Appl Polym Sci* 1986; 31: 535–551. John Wiley & Sons, Ltd.
- Ohlsson B, Hassander H and Törnell B. Improved compatibility between polyamide and polypropylene by the use of maleic anhydride grafted SEBS. *Polymer* 1998; 39: 6705–6714. Elsevier.
- Sharma R and Maiti SN. Melt rheological properties of PBT/SEBS and reatively compatibilized PBT/SEBS/SEBS-g-MA polymer blends. *J Appl Polym Sci* 2015; 132: 41402. John Wiley & Sons, Ltd.
- Gopalan AM and Naskar K. Ultra-high molecular weight styrenic block copolymer/TPU blends for automotive applications: influence of various compatibilizers. *Polym Adv Technol* 2019; 30: 608–619. John Wiley & Sons, Ltd.
- Parameswaranpillai J, Jose S, Siengchin S, et al. Phase morphology, mechanical, dynamic mechanical, crystallization, and thermal degradation properties of PP and PP/PS blends modified with SEBS elastomer. *Int J Plast Technol* 2017; 21: 79–95. Springer India.
- Wu T, Hu Y, Rong H, et al. SEBS-based composite phase change material with thermal shape memory for thermal management applications. *Energy* 2021; 221: 119900. Pergamon.
- Gennari CGM, Quaroni GMG, Creton C, et al. SEBS Block copolymers as novel materials to design transdermal patches. *Int J Pharm* 2020; 575: 118975. Elsevier.
- Elisa M, Giancarlo G, Dory C, et al. Wettability and surface tension of amphiphilic polymer films: time-dependent measurements of the most stable contact angle. *Macromol Chem Phys* 2012; 213: 1448–1456. John Wiley & Sons, Ltd.
- Micheletti C, Dini VA, Carlotti M, et al. Blending or bonding? Mechanochromism of an aggregachromic mechanophore in a thermoplastic elastomer. *ACS Applied Polymer Materials* 2023; 5: 1545–1555. American Chemical Society.
- Knuschke P. UV Exposure. In: *Kanerva's occupational dermatology*. Cham: Springer, 2020, pp.1145–1178.
- Reed NG. The history of ultraviolet germicidal irradiation for air disinfection. 2010; 125: 15–27. <http://dx.doi.org/10.1177/003335491012500105>. SAGE PublicationsSage CA: Los Angeles, CA.
- Brenneisen P, Sies H and Scharffetter-Kochanek K. Ultraviolet-B irradiation and matrix metalloproteinases. *Ann N Y Acad Sci* 2002; 973: 31–43. John Wiley & Sons, Ltd.
- Dai T, Vrahas MS, Murray CK, et al. Ultraviolet C irradiation: an alternative antimicrobial approach to localized infections? *Expert Rev Anti-Infect Ther* 2012; 10: 185–195. Taylor & Francis.
- Ceretti DVA, Edeleva M, Cardon L, et al. Molecular pathways for polymer degradation during conventional processing, additive manufacturing, and mechanical recycling.

- Molecules* 2023; 28: 2344. Multidisciplinary Digital Publishing Institute.
- 25. Alavi K, Tarashi S, Nazockdast H, et al. Microstructure development and mechanical performance of MWCNTs/GNPs filled SEBS with different block content. *Polym Compos* 2023; 44: 8125–8140. John Wiley & Sons, Ltd.
  - 26. de Sousa RR, Sacramento JB, da Silva LCE, et al. High-performance block-copolymer-based dielectric elastomers with enhanced mechanical properties. *ACS Appl Polymer Mater* 2023; 5: 9505–9514. American Chemical Society.
  - 27. Zhang Q, Hua W, Ren Q, et al. Regulation of physical networks and mechanical properties of triblock thermoplastic elastomer through introduction of midblock similar crystalline polymer with multiblock architecture. *Macromolecules* 2016; 49: 7379–7386. American Chemical Society.
  - 28. Angelo RJ, Ikeda RM and Wallach ML. Multiple glass transitions of block polymers. *Polymer* 1965; 6: 141–156. Elsevier.
  - 29. Daimon H, Okitsu H and Kumanotani J. Glass transition behaviors of random and block copolymers and polymer blends of styrene and cyclododecyl acrylate. I. Glass transition temperatures. *Polym J* 1975; 7: 460–466. Nature Publishing Group.
  - 30. Song X, Wang W, Yang F, et al. The study of enhancement of magnetorheological effect based on natural rubber/thermoplastic elastomer SEBS hybrid matrix. *J Intell Mater Syst Struct* 2020; 31: 339–348. SAGE Publications Ltd.
  - 31. Banerjee SS, Burbine S, Shivaprakash NK, et al. 3D-printable PP/SEBS thermoplastic elastomeric blends: preparation and properties. *Polymers (Basel)* 2019; 11: 347. Multidisciplinary Digital Publishing Institute.
  - 32. Gao W, Yu B, Li S, et al. Preparation and properties of reinforced SEBS-based thermoplastic elastomers modified by PA6. *Polymer Eng Sci* 2022; 62: 1052–1060. John Wiley & Sons, Ltd.
  - 33. Allen NS, Edge M, Wilkinson A, et al. Degradation and stabilisation of styrene–ethylene–butadiene–styrene (SEBS) block copolymer. *Polym Degrad Stab* 2000; 71: 113–122. Elsevier.
  - 34. Allen NS, Luengo C, Edge M, et al. Photooxidation of styrene–ethylene–butadiene–styrene (SEBS) block copolymer. *J Photochem Photobiol A* 2004; 162: 41–51. Elsevier.
  - 35. Allen NS, Edge M, Mourelatou D, et al. Influence of ozone on styrene–ethylene–butylene–styrene (SEBS) copolymer. *Polym Degrad Stab* 2003; 79: 297–307. Elsevier.
  - 36. White CC, Tan KT, Hunston DL, et al. Laboratory accelerated and natural weathering of styrene–ethylene–butylene–styrene (SEBS) block copolymer. *Polym Degrad Stab* 2011; 96: 1104–1110. Elsevier.
  - 37. Kusmono M, Ishak ZA, Chow WS, et al. Influence of SEBS-g-MA on morphology, mechanical, and thermal properties of PA6/PP/organoclay nanocomposites. *Eur Polym J* 2008; 44: 1023–1039. Pergamon.
  - 38. Ujcic M, Levak M, Vranjes Penava N, et al. Thermal degradation and thermal kinetic of SEBS block copolymer compatibilized PS/HDPE blends. *J Elastomers Plast* 2023; 55: 82–98.
  - 39. Zulfiqar S, Ahmad Z, Ishaq M, et al. Thermal and mechanical properties of SEBS-g-MA based inorganic composite materials. *J Mater Sci* 2007; 42: 93–100. Springer.
  - 40. Parameswaranpillai J, Joseph G, Shinu KP, et al. High performance PP/SEBS/CNF composites: evaluation of mechanical, thermal degradation, and crystallization properties. *Polym Compos* 2017; 38: 2440–2449. John Wiley & Sons, Ltd.
  - 41. Peinado C, Corrales T, Catalina F, et al. Effects of ozone in surface modification and thermal stability of SEBS block copolymers. *Polym Degrad Stab* 2010; 95: 975–986. Elsevier.
  - 42. Chriaa I, Trigui A, Karkri M, et al. Thermal properties of shape-stabilized phase change materials based on low density polyethylene, hexadecane and SEBS for thermal energy storage. *Appl Therm Eng* 2020; 171: 115072. Pergamon.
  - 43. Nehra R, Maiti SN and Jacob J. Analytical interpretations of static and dynamic mechanical properties of thermoplastic elastomer toughened PLA blends. *J Appl Polym Sci* 2018; 135: 45644. John Wiley & Sons, Ltd.
  - 44. Karode NS, Poudel A, Fitzhenry L, et al. Evaluation of interfacial region of microphase-separated SEBS using modulated differential scanning calorimetry and dynamic mechanical thermal analysis. *Polym Test* 2017; 62: 268–277. Elsevier.